Catalysis Letters 38 (1996) 189–195

Oxidative dehydrogenation of ethane over $La_{1-x}Sr_xFeO_{3-\delta}$ perovskite oxides

Guanghua Yi [1], Takashi Hayakawa, Arnfinn G. Andersen [a,2], Kunio Suzuki, Satoshi Hamakawa, Andrew P.E. York, Masao Shimizu and Katsuomi Takehira [2]

Department of Surface Chemistry, National Institute of Materials and Chemical Research, Higashi 1-1, Tsukuba, Ibaraki 305, Japan
[a] Nycomed Imaging AS, PO Box 4220, Torshov, 0401 Oslo, Norway

Received 17 August 1995; accepted 18 January 1996

Catalysts of the composition $La_{1-x}Sr_xFeO_{3-\delta}$, $0 \leqslant x \leqslant 1$, have been tested for the oxidative dehydrogenation of ethane in the temperature range 300–800°C. The catalyst is active above 400°C, giving a maximum yield of 37% ethylene at 650°C. Above 650°C, synthesis gas was formed together with methane, suggesting that the reforming reaction and thermal cracking of ethane took place. The catalytic data are compared to conductivity measurements on the same material, and a good correlation between the activity and p-type conductivity has been found. In the phase diagram for the system $LaFeO_3$–$SrFeO_{3-\delta}$, a phase separation to two types of (La, Sr)$FeO_{3-\delta}$ perovskites was observed in the La/Sr binary composition in the temperature range below 800°C. The phase separation can elucidate the dependency of the catalytic activity on its p-type conductivity.

Keywords: perovskite; $La_{1-x}Sr_xFeO_{3-\delta}$; dehydrogenation; oxidation; ethane

1. Introduction

We have previously reported the catalytic reactions of light hydrocarbons over several perovskite oxides [1]. These materials are of interest since they are chemically and mechanically stable under various conditions, and show various types of conductivity and defect structures [2]. An important feature is the possibility of large variations in oxygen content. In this respect, perovskites may provide a surface with large oxygen capacity for oxidative reactions [3]. Perovskites are also among the most promising materials for membrane reactors of various kinds and fuel cell electrodes [3,4].

In the (La, Sr)$FeO_{3-\delta}$ system, p-type conductivity is expected under oxidative conditions, with lowest conductivity for pure $LaFeO_3$ [5]. The variation of conductivity with Sr-content, temperature and oxygen partial pressure is widely studied in the literature [6], but no such data are available for temperatures below 800°C, where most catalytic reactions take place. It has also been shown that phase separation can occur below 1000°C in the (La, Sr)$FeO_{3-\delta}$ system [6]. Above this temperature, La and Sr are totally interchangeable on A-sites in the perovskite lattice.

Cameron et al. [7] reported that p-type conductivity is an important feature for the activity of a catalyst for the oxidative coupling of methane (OCM), which gives ethylene and CO_2 as the main products. We have also previously reported this phenomenon both for the OCM and the oxidative dehydrogenation of ethane, in the system (Ca, Sr)(Fe,Ti)$O_{3-\delta}$ [8]. One of the authors has also mentioned the importance of the p-type conductivity of Li : MgO catalysts often used for the OCM reaction [9].

Here we report the catalytic activity of (La, Sr)$FeO_{3-\delta}$ perovskites for the oxidative dehydrogenation of ethane related to the phase diagram and the electric conductivity.

2. Experimental

2.1. Preparation of the catalyst

(La, Sr)$FeO_{3-\delta}$ perovskite oxides were prepared by the thermal decomposition of precursor complexes derived from nitrate solutions using ethylenediaminetetraacetic acid (EDTA) as a complexing agent [4]. The metal nitrates, $La(NO_3)_3 \cdot 6H_2O$ (Soekawa Chem.) and $Fe(NO_3)_3 \cdot 9H_2O$ (Soekawa Chem.), and strontium carbonate $SrCO_3$ (Soekawa Chem.) were dissolved in stoichiometric ratios in distilled water under heating at about 80°C. Then, EDTA (Kanto Chem.) was added as a chelating agent. 1.5 mole of EDTA was used for each mole of metal. By adding ammonia water to the mixture, to keep the pH above 7, a red solution was formed. The solution was then heated on a hot plate to remove the water and a uniform gel was obtained. The gel was pyrolyzed by further heating at about 250°C on the hot plate. The pyrolyzed gel was then ground and calcined at 1000°C for 8 h in air. Cooling was performed by turning off the furnace. The samples with compositions $La_{1-x}Sr_xFeO_{3-\delta}$, where $x = 0$, 0.1, 0.2, 0.35, 0.5, 0.65,

[1] Present address: Department of Physics, Hong Kong University of Science and Technology, Clear Water Bay, Kowloon, Hong Kong.
[2] To whom correspondence should be addressed.

0.8, 0.9 and 1, were prepared using this method. The samples were then characterized by XRD.

2.2. Catalytic testing

The samples prepared by the above method were tested in a fixed bed catalyst reactor using a gaseous mixture of ethane (0.34 ℓh^{-1}) and air (1.66 ℓh^{-1}), corresponding to an ethane to O_2 molar ratio of 1/1. 300 mg catalyst was dispersed in quartz wool to avoid sintering and clogging of the reactor. A U-shaped quartz reactor was used (i.d. 10 mm), with the catalyst bed near the bottom. A thermocouple was introduced from the top of the reactor and placed in the middle of the catalyst bed. All reaction products were analyzed by gas chromatography.

The temperature of the reactor was first raised to 200°C in air and the reactant gas mixture was introduced after a short flushing with nitrogen gas. The temperature was further elevated to 850°C in stepwise increments of 50°C, and no change in the product distributions was observed after 15 min on line at each temperature. All samples were taken after establishing the steady state reaction and analyzed by gas chromatography. After finishing the catalytic tests, the reaction mixture was replaced with nitrogen gas and the reactor was cooled down by removing it from the furnace. The catalysts were then removed from the reactor and characterised by XRD.

2.3. Conductivity measurements

1 g of the perovskite powder was pressed into a tablet (13 mm diameter and 1 mm thick) with a pressure of 1800 kg/cm^2 for 20 min. In order to avoid cracking of the tablet, a drop of glycerol was mixed with the powder as a binder before pressing. The tablets were then sintered at 1100°C for 6 h in air.

For Seebeck coefficient measurements, two thermocouples spaced 6 mm apart, were pressed onto the tablet by a spring. The potential difference between the Pt legs of the two thermocouples was measured and the temperature difference between the two Pt legs, created by passing a DC current through a Ni/Cr coil wound round the alumina tube of one thermocouple, was determined. The conductivity of the tablet was then calculated from the measured resistance and the geometrical factor for the two-probe measurement of the tablet. In order to obtain the geometrical factor, a rectangular sample (1.8 mm by 3.3 mm in cross section and 7.0 mm long) was cut from a tablet with a composition of $La_{0.8}Sr_{0.2}FeO_{3-\delta}$. The conductivity of the sample was then measured with a standard DC four-probe method at different temperatures. The geometrical factor was obtained by comparing the resistance measured on a tablet of the same composition as the rectangular sample by the two-probe method with the conductivity measured by the standard four-probe method.

2.4. Characterization of the catalyst

The powder X-ray diffraction (XRD) patterns of the catalyst were recorded using a MXP-18 (MAC Science Co.) with Cu Kα radiation. Thermal analyses (TGA/DTA) were carried out using a Shimadzu TGA 50 and DTA 50 containing an electrobalance. The conductivity of the catalyst was measured with a Hewlett-Packard 3478 A multimeter. A digital multi-thermometer from Advantest and a pair of Pt/PtRh thermocouples were used to measure the temperature of the samples.

3. Results

3.1. Catalytic testing

Samples of all compositions mentioned above were tested for the ethane oxidation. Representative data from the catalytic testing of these materials are given in figs. 1, 2 and 3, all of which illustrate typical conversions and selectivities as a function of temperature. Figs. 1 and 2 show the results for the two samples of extreme compositions, i.e. $LaFeO_3$ and $SrFeO_{3-\delta}$, while fig. 3 gives an example of an intermediate composition, in this case $La_{0.5}Sr_{0.5}FeO_{3-\delta}$. All of the La–Sr mixed oxides showed similar features of the product formation to the $La_{0.5}Sr_{0.5}FeO_{3-\delta}$. The oxygen conversion rose abruptly around 400°C, and the ethane conversion followed duly. The rise in conversion occurred at lower temperatures for compositions with $0.1 \leqslant x \leqslant 0.9$ than for the extreme compositions, $LaFeO_3$ and $SrFeO_{3-\delta}$, both of which gave the rapid oxygen conversion around 500°C. At lower temperatures, CO_2 was the only product, but the ethene selectivity increased with temperature and reached a substantial amount at 650°C. For $SrFeO_{3-\delta}$, the highest ethene selectivity of 43% was observed at an ethane conversion of 87%, giving an ethene yield of 37%.

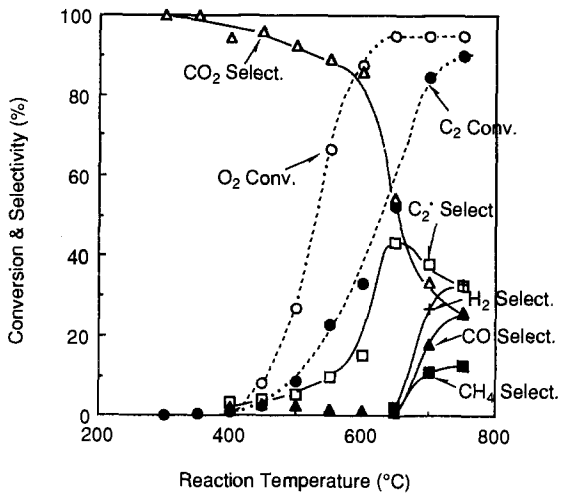

Fig. 1. Ethane oxidation over $LaFeO_3$ catalyst.

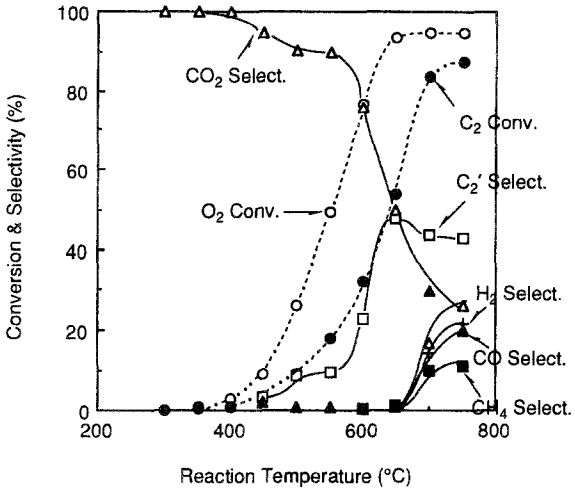

Fig. 2. Ethane oxidation over $SrFeO_{3-\delta}$ catalyst.

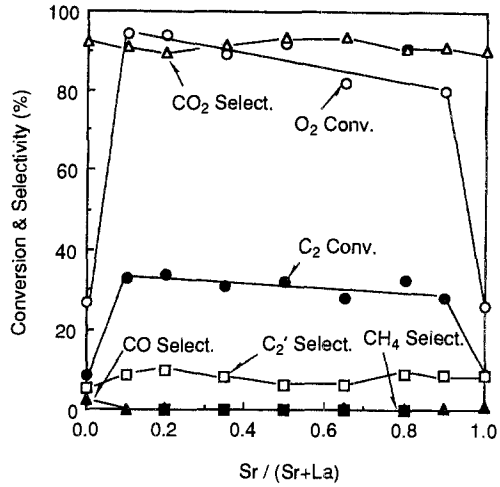

Fig. 4. Ethane oxidation over $La_{1-x}Sr_xFeO_{3-\delta}$ catalyst at 500°C.

For all the samples, CO and H_2 were formed above 650°C, the amounts increasing with temperature. Methane was also observed to increase in the same temperature range. These observations are accompanied by the "second step" above 650°C in the ethane conversion curve as seen in fig. 3. The two steps in the ethane conversion curve were of the same magnitude and the second step started at the same temperature for all catalysts with $0.1 \leqslant x \leqslant 0.9$. A comparison of catalytic properties between all the samples at 500°C is shown in fig. 4, where conversions and selectivities are plotted as a function of catalyst composition. Both the oxygen and ethane conversions showed a volcano type dependency on the compositions; La–Sr binary type perovskite oxides showed a higher activity for the ethane oxidation than the $LaFeO_3$ and $SrFeO_{3-\delta}$ perovskites.

3.2. *Conductivity measurements*

Typical conductivity measurement results for several of the samples are plotted as $\log \sigma$ versus inverse temperature (fig. 5). This plot has often been used for investigating the conduction mechanism and the activation energy connected to conduction [5]. In the present study, we used the same presentation in order to ease the comparison with the literature data [5].

Our observations are in good agreement with the conclusions in the literature, i.e. that the material is a p-type conductor at all the catalyst compositions under high oxygen partial pressures and/or lower temperatures [5]. p-type conductivity was confirmed by a positive Seebeck effect. The conductivity increased in all the samples up to about 500°C in air; further heating normally caused a constant or slightly decreasing conductivity. The latter phenomenon is normally related to metallic conduction mechanisms. The shapes of the curves are comparable to the data of Poulsen et al. [10]. There seems to be a systematic change in the activation energy for conduction in the lower temperature region, where intermediate compositions show the lowest activation energy, but it is out of the scope of this study to elaborate further on this phenomenon. Log σ of $LaFeO_3$, which was extremely low compared to the others,

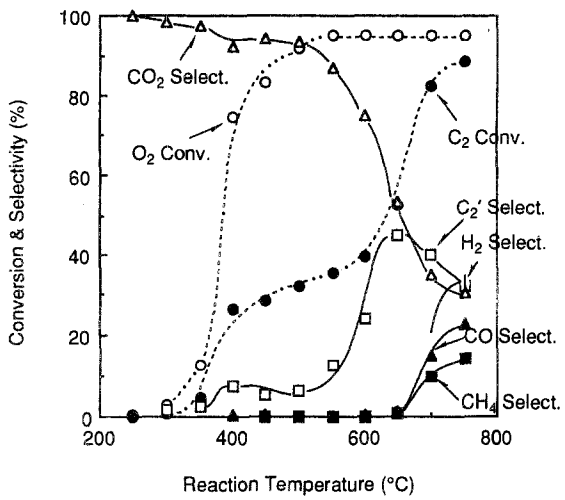

Fig. 3. Ethane oxidation over $La_{0.5}Sr_{0.5}FeO_{3-\delta}$ catalyst.

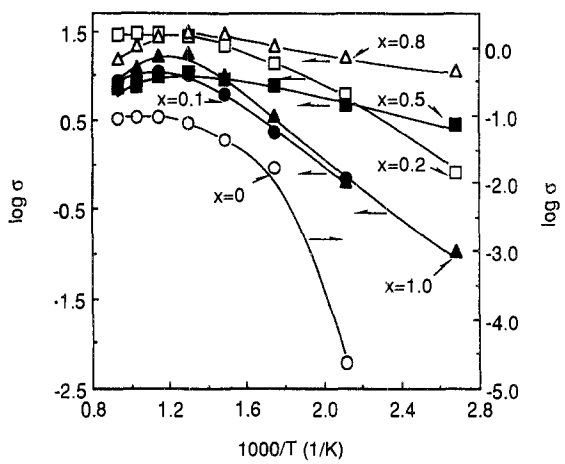

Fig. 5. Conductivity (p-type) of $La_{1-x}Sr_xFeO_{3-\delta}$ in air.

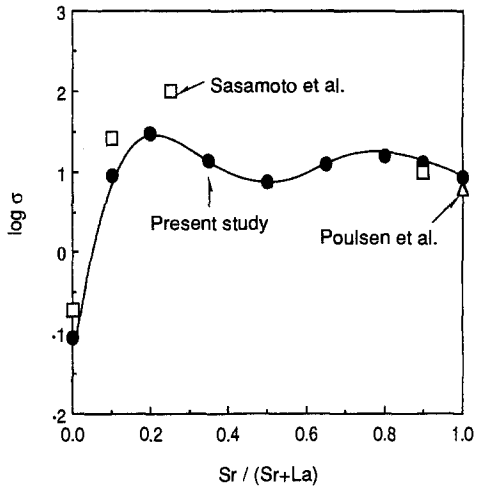

Fig. 6. Conductivity of $La_{1-x}Sr_xFeO_{3-\delta}$ at 800°C in air. Including the data of Sasamoto [6] (squares) and Poulsen [10] (triangle). The data from the present study are given as filled circles.

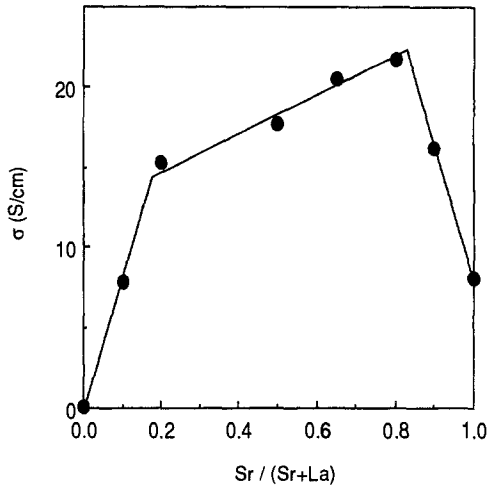

Fig. 8. Conductivity of $La_{1-x}Sr_xFeO_{3-\delta}$ in ethane and air (1 : 1) at 500°C.

increased with temperature and reached a maximum value of −1.0 at 700°C. The activation energy for this compound was in the same range as for $x = 0.1$. Values of $\log \sigma$ obtained with the $La_{1-x}Sr_xFeO_{3-\delta}$ at 800°C in air were plotted as a function of the compositions (fig. 6). At this temperature, the present data can be compared with those reported previously by Sasamoto [6] and Poulsen [10], resulting in a good agreement between each other. At temperatures above 650°C and in the mixed gas used for the catalytic testing, the conductivity of the samples decreased dramatically, as shown in fig. 7. In the same temperature region, the gaseous products from the catalytic reactor also changed, as seen in fig. 3. Fig. 8 shows the conductivity (σ) of the $La_{1-x}Sr_xFeO_{3-\delta}$ at 500°C in the mixture of ethane and air. No reduction of the catalyst and no synthesis gas production was observed under these conditions.

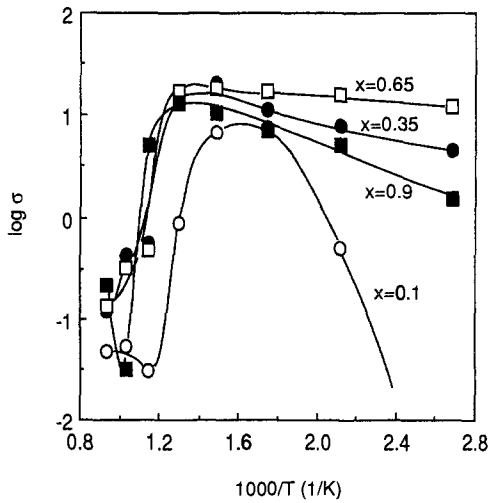

Fig. 7. Conductivity of $La_{1-x}Sr_xFeO_{3-\delta}$ in ethane and air (1 : 1).

3.3. X-ray observations

The X-ray diffraction patterns of the samples after the synthesis show the presence of $LaFeO_3$ and $SrFeO_{3-\delta}$ for both extreme compositions (fig. 9). These diffraction patterns are quite similar to each other due to the close link between their crystal structures, i.e. orthorhombic $LaFeO_3$ (JCPDS 37-1493) and cubic $SrFeO_{3-\delta}$ (JCPDS 34-638). It has been reported that both brownmillerrite, $SrFeO_{2.5}$, and cubic $SrFeO_{3-\delta}$ can form at 400–900°C, while cubic $SrFeO_{3-\delta}$ appears alone above 900°C [11]. For compositions of $La_{1-x}Sr_xFeO_{3-\delta}$ with $0.2 \leqslant x \leqslant 0.8$, the diffractograms showed double peaks with overlapping and shoulders (fig. 9), though resolution of the peaks was not possible due to the limitations of our instrument. The samples after the reaction showed no distinct change from those after synthesis, suggesting

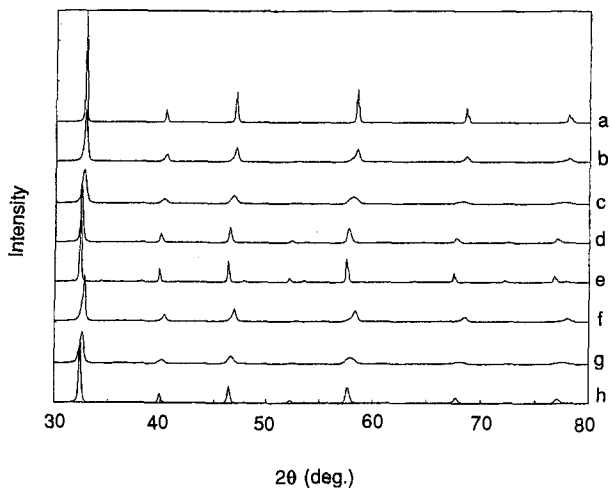

Fig. 9. X-ray diffractograms of $La_{1-x}Sr_xFeO_{3-\delta}$ before and after the reaction: (a) $LaFeO_3$ (before), (b) $La_{0.75}Sr_{0.35}FeO_{3-\delta}$ (before), (c) $La_{0.5}Sr_{0.5}FeO_{3-\delta}$ (before), (d) $La_{0.2}Sr_{0.8}FeO_{3-\delta}$ (before), (e) $SrFeO_{3-\delta}$ (before), (f) $La_{0.75}Sr_{0.35}FeO_{3-\delta}$ (after), (g) $La_{0.5}Sr_{0.5}FeO_{3-\delta}$ (after), (h) $La_{0.2}Sr_{0.8}FeO_{3-\delta}$ (after).

that no substantial change took place in the crystal structure during the reaction. Fig. 10 illustrates the diffractograms of $La_{0.5}Sr_{0.5}FeO_{3-\delta}$ for 2θ in the range 75–80°. Sample a calcined at 1000°C for 8 h followed by slow cooling showed a broad line, probably of the double peaks, due to the formation of two phases. Sample b equilibrated at 800°C for 24 h and quenched by quick cooling showed a similar peak as the sample a. However, sample c calcined at 1150°C for 4 h and then quenched by quick cooling gave the peak from a single phase. The X-ray diffraction thus confirms the presence of two phases at lower calcination temperature (800°C) (b) or without quenching (a). The samples cooled by turning off the furnace therefore represent the situation at lower temperature.

3.4. Thermal analysis

Thermogravimetry of materials in the range $La_{1-x}Sr_xFeO_{3-\delta}$ has been reported in the literature as a function of partial pressure of oxygen at fixed temperatures [12]. We have previously reported traditional TGA studies of $SrFeO_{3-\delta}$ in air and nitrogen as a function of temperature [1b]. In the present study, we reconfirmed that $SrFeO_{3-\delta}$ easily gives off oxygen upon heating in air, and that this ability decreases with increasing the lanthanum content of the catalyst. These observations are in fair agreement with the oxygen content at various temperatures reported by Takeda et al. [13].

Differential thermal analysis (DTA) was performed on the samples of $La_{1-x}Sr_xFeO_{3-\delta}$ with $0.1 \leqslant x \leqslant 0.9$ from room temperature to 1200°C in air. According to the literature [6], the solidus and liquidus for this system is expected at 1300–1800°C. The samples cooled slowly to room temperature gave no signal in DTA during the heating. The samples quenched from above 1100°C gave a weak exothermal signal upon heating at the rate of 10°C/min in the range 800–1100°C (fig. 11). It is known that the single phase perovskite in this system is easily quenched from high temperatures at any composition [6]. No signals could be observed for the samples with $x = 0.1$ and $x = 0.9$, probably because the system is close to single phase throughout the whole heating procedure. A possible phase transition will also occur at very low temperatures for DTA studies of these samples. No DTA peaks could be observed during cooling.

A phase separation below 1000°C has been suggested in a tentative binary phase diagram of the system $LaFeO_3$–$SrFeO_{3-\delta}$ by Sasamoto et al. [6], based on an XRD study. The observations of Sasamoto et al. are included in the phase diagram for the system $LaFeO_3$–$SrFeO_{3-\delta}$ given in fig. 12, where the solid state phase separation is based on our DTA measurements. The end points of the exothermal peaks in DTA (fig. 11) are taken to represent the single phase boundary. The liquidus and solidus in the same figure are taken from Sasamoto et al. [6]. In the present study, an endothermal peak was expected during heating across the two-phase line. However, this reaction is diffusion limited and probably too slow to give an observable DTA peak. The exothermal peak observed for quenched samples could be related to a relaxation in the crystallites when returning to stable single phase conditions.

4. Discussion

The results in this study should be interpreted remembering that there is a two-phase situation in most of the intermediate compositions of the catalyst. The extension of the single phase boundaries at lower temperatures have not been confirmed by our experiments, but it may

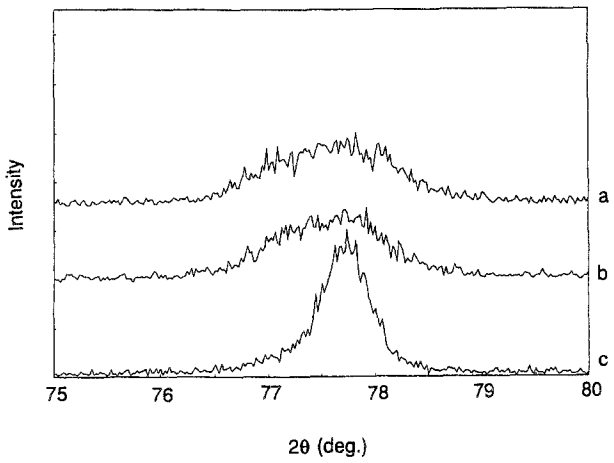

Fig. 10. X-ray diffractograms of $La_{1-x}Sr_xFeO_{3-\delta}$ in the region $75° < 2\theta < 80°$. (a) Calcined at 1000°C for 8 h followed by slow cooling, (b) equilibrated at 800°C for 24 h and quenched by quick cooling, (c) calcined at 1150°C for 4 h and then quenched by quick cooling.

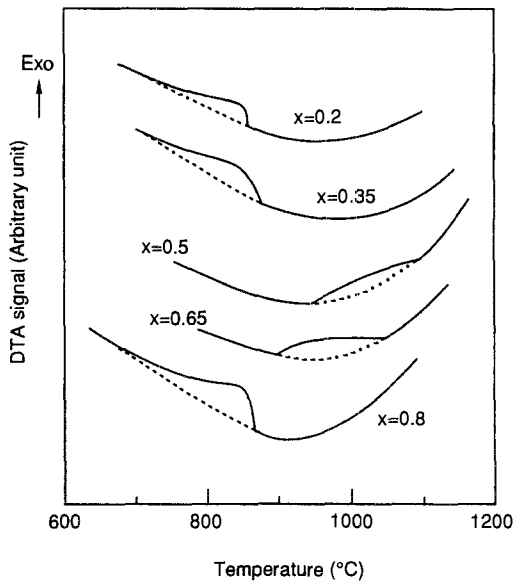

Fig. 11. DTA curves of $La_{1-x}Sr_xFeO_{3-\delta}$ ($0.2 \leqslant x \leqslant 0.8$). The heating rate was 10°C/min. Air was flowing constantly over the sample.

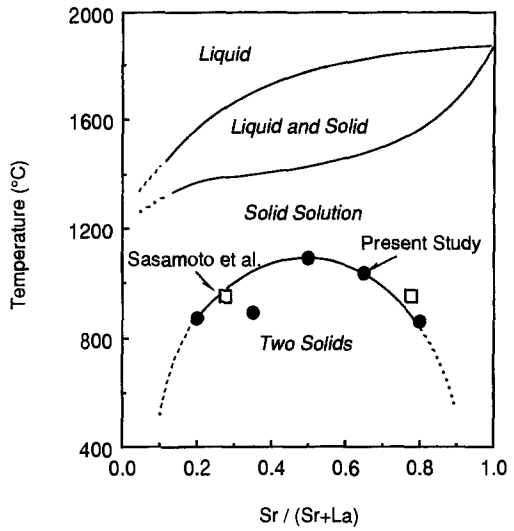

Fig. 12. Phase diagram for the system $LaFeO_3$–$SrFeO_{3-\delta}$. The data is based on the observations of Sasamoto et al. [6] (squares in addition to liquidus and solidus) and the present study (filled circles).

be easy to extrapolate the curves in fig. 12 to get approximate figures. At a given temperature, e.g. 600°C, $LaFeO_3$ may dissolve Sr on A-sites in the lattice to a composition close to $La_{0.9}Sr_{0.1}FeO_{3-\delta}$. The situation is similar starting with $SrFeO_{3-\delta}$ where La may replace Sr on A-sites to a similar extent. In the region between these, i.e. for approximately $0.1 < x < 0.9$, the catalyst will consist of a mixture of the two phases. At a given temperature and in air, the conductivity is expected to change with composition inside a single phase area, due to doping and variation in the concentration of point defects and mobile electrons/holes. With compositions in the two-phase region, the conductivity will be an interpolation of the end points at the phase boundaries, possibly modified with some interfacial contact effects.

The catalytic features in the single phase region are expected to change as a function of the composition at a given temperature for the same reason as above. From the literature, one would also expect variation in the catalytic activity in the two-phase region due to synergies, phase interactions and surface modification, etc. Apart from this, it is likely that the result of the catalytic testing in the two-phase region is an interpolation of the end points of the single phases. From the data in figs. 4, 8 and 12, there seems to be a good correlation between the catalytic activity, the p-type conductivity and the phase separation. The perovskites used in the present study show high conductivity for oxide ions at high Sr contents and low conductivity for $LaFeO_3$ [5], showing no correlation between oxide ionic conductivity and catalytic activity. The same argument could be used for oxygen vacancies, which are expected to be of importance for oxidation reactions. This good correlation between the p-type conductivity and the catalytic activity in ethane oxidation agrees with our previous observations for other perovskites [8]. It is also in agreement with the assumptions of Cameron et al. concerning the OCM reaction [7]. Furthermore, the catalytic tests and the conductivity measurements in the two-phase region at 500°C may be interpreted as an interpolation of the values at $x = 0.1$ and $x = 0.9$.

Above 650°C, the main product was still ethene, but the amount of CO and H_2 increased with temperature. This is probably related to a reduction of the catalyst surface to yield metallic iron over the catalyst. As the ethene selectivity is not dramatically altered, the reduction seems to be incomplete. No distinct change was observed in the XRD patterns after the reaction, suggesting that no substantial change took place in the crystal structure during the reaction. The conductivity of the sample under the same conditions was dramatically reduced. The results above 650°C can be interpreted as a production of synthesis gas by complete oxidation followed by reforming of ethane over metallic iron. A similar phenomenon has been observed over the (Ca, Sr)(Co,Ti)$O_{3-\delta}$ perovskite [14], where the distribution of products more dramatically changed below and above the reduction temperature. The literature also shows similar examples for $LaCoO_3$ and $LaRhO_3$ [15]. The H_2/CO ratio in the present study is lower than expected for the mentioned reactions to synthesis gas above 650°C. This may be interpreted by the difference between the rates of oxidation of the respective molecules. Van Hassel et al. [4] have recently reported that the oxidation of CO on the surface of a $La_{1-x}Sr_xFeO_{3-\delta}$ membrane is limiting the transport of oxygen through the membrane. Diffusion of oxide ion vacancies was determined with $La_{1-x}Sr_xFeO_{3-\delta}$ by using an ^{18}O tracer method [16]. No exact data for the oxidation rate is given, but one may assume that H_2 is more rapidly oxidized than CO over the present perovskite.

No thermodynamic data concerning the reduction of $La_{1-x}Sr_xFeO_{3-\delta}$ under a low oxygen pressure is given in the literature. Mizusaki et al. [5] have reported conductivity measurements in equilibrated mixtures of CO and CO_2 at higher temperatures down to oxygen partial pressures of 10^{-10} Pa (1100°C) or 10^{-15} Pa (900°C). The lowest pressure in these measurements has been normally given by the starting of reduction of the sample. In the present study, equilibrium was not established in the gas phase. However, assuming equilibrium between CO/CO_2 (average ratio is 0.5 at 700°C in the present study) yields a partial pressure of oxygen about 10^{-25} Pa at 700°C. From these figures, it seems reasonable to assume that the catalyst surface may be partly reduced under the conditions at higher temperatures in this study.

5. Conclusion

Several compositions of $La_{1-x}Sr_xFeO_{3-\delta}$ have been tested for oxidative dehydrogenation of ethane in the

temperature region 300–800°C. The activity of the catalysts rose around 400°C and the main product was CO_2 at lower temperatures. The ethene selectivity increased with increasing temperature and reached the highest value at 650°C. Above 650°C, synthesis gas and methane were formed over the catalyst. The activity of the catalyst seems to be correlated to the p-type conductivity of the material. A phase separation between Sr-rich and La-rich perovskites is observed by DTA and XRD. This separation was reflected in both the conductivity and the catalytic activity.

Acknowledgement

The authors wish to thank Drs. H. Yokokawa and N. Sakai of NIMC for helpful discussions and thermodynamic calculations.

References

[1] (a) T. Hayakawa, A.G. Andersen, H. Orita, M. Shimizu and K. Takehira, Catal. Lett. 16 (1992) 373;
A.G. Andersen, T. Hayakawa, M. Shimizu, K. Suzuki and K. Takehira, Catal. Lett. 23 (1994) 59.
(b) A.G. Andersen, T. Hayakawa, T. Tsunoda, H. Orita, M. Shimizu, K. Suzuki and K. Takehira, Catal. Lett. 18 (1993) 37.

[2] M. Misono and E.A. Lombardo, eds., *Perovskites*, Catal. Today 8 (1990) pp. 133–275.

[3] T. Seiyama, Catal. Rev. Sci. Eng. 34 (1992) 281;
T. Shimizu, Catal. Rev. Sci. Eng. 34 (1992) 355.

[4] B.A. van Hassel, J.E. ten Elshof and H.J.M. Bouwmeester, Appl. Catal. A 119 (1994) 279.

[5] J. Mizusaki, T. Sasamoto, W.R. Cannon and H.K. Bowen, J. Am. Ceram. Soc. 65 (1982) 363; 66 (1983) 247;
K. Gaur, S.C. Verma and H.B. Lal, J. Mater. Sci. 23 (1988) 1725.

[6] T. Sasamoto, J. Mizusaki, M. Yoshimura, W.R. Cannon and H.K. Bowen, Yogyo-Kyokai-Shi 90 (1982) 24.

[7] J.-L. Dubois and C.J. Cameron, Appl. Catal. 67 (1990) 49.

[8] T. Hayakawa, A.G. Andersen, H. Orita, M. Shimizu and K. Takehira, Catal. Lett. 16 (1992) 373;
A.G. Andersen, T. Hayakawa, M. Shimizu, K. Suzuki and K. Takehira, Catal. Lett. 23 (1994) 59.

[9] T. Norby and A.G. Andersen, Appl. Catal. 71 (1991) 89.

[10] F.W. Poulsen, G. Lauvstad and R. Tunold, *Proc. 9th Solid State Ionics Conference*, The Hague, September 1993.

[11] J. Mizusaki, M. Okayasu, S. Yamauchi and K. Fueki, J. Solid State Chem. 99 (1992) 166.

[12] J. Mizusaki, M. Yoshihiro, S. Yamauchi and K. Fueki, J. Solid State Chem. 58 (1985) 257.

[13] Y. Takeda, K. Kanno, T. Takada, O. Yamamoto, M. Takano, N. Nakayama and Y. Bando, J. Solid State Chem. 63 (1986) 237.

[14] T. Hayakawa, A.G. Andersen, M. Shimizu, K. Suzuki and K. Takehira, Catal. Lett. 22 (1993) 307.

[15] A. Slagtern and U. Olsbye, Appl. Catal. A 110 (1994) 99.

[16] T. Ishigaki, S. Yamauchi, K. Kishio, J. Mizusaki and K. Fueki, J. Solid State Chem. 73 (1988) 179.